A 10V compliant 16-channel stimulator ASIC with sub-10nA mismatch and simultaneous ETI sensing for selective vagus nerve stimulation

Haoming Xin*[1], Meiyi Zhou*[1], Roland van Wegberg[1], Peter Vis[1], Konstantinos Petkos[1], Shrishail Patki[1], Nicolo Rossetti[1], Mark Fichman[1], Vojkan Mihajlovic[1], Carolina Mora Lopez[2], Geert Langereis[1], Mario Konijnenburg[1], Nick Van Helleputte[2]

[1]imec-Netherlands, the Netherlands [2] IMEC, Belgium

*Equally Credited Authors

The vagus nerve (VN) is a key part of the parasympathetic nervous system connecting the brain to various organs. VN stimulation has been FDA-approved for treatment of drug-resistant epilepsy and depression and holds promise for chronic inflammation and arrythmia [1]. However, existing solutions either have poor spatial selectivity causing unwanted side effects or incur a high risk for nerve damage (Fig.1). This work proposes non-penetrating high-density cuff electrodes driven by an ASIC that employs temporal interference stimulation (TIS) [2] to improve spatial selectivity (Fig.1). In TIS, a pair of differential current stimulators generates two kHz-range semi-continuous sinusoidal currents with a small frequency offset (e.g. 10Hz). This creates an interference pattern within the tissue. Since neural cells are more receptive to low-frequency (LF), they would be entrained by the LF envelope. The stimulation intensity of the LF envelope can be steered to any location by selecting different electrode pairs and/or stimulation current amplitudes [2].

Besides spatial selectivity, a VN stimulator IC must meet 3 crucial requirements: i) delivery of large stimulation currents (up to 10mA for certain therapies [1]) with small cuff electrodes (~kΩ impedance), which requires a high voltage (HV) compliance (≥10V); ii) charge-balancing (CB) to avoid electrode or tissue damage due to charge accumulation; and iii) electrode-tissue impedance (ETI) sensing during stimulation which provides critical clinical information. However, due to the semi-continuous nature of TIS (Fig. 1), existing CB and ETI approaches for biphasic stimulators are not applicable. While an TIS IC has been demonstrated [3], it has a low compliance voltage (3.3V), does not implement active CB, nor allow ETI sensing during TIS. To tackle these challenges, we present a HV TIS IC with on-the-fly active CB and ETI sensing during the stimulation.

TIS requires at least 2 bipolar sinusoidal current stimulators with adjustable amplitudes and electrode selection to enable focal steering [2]. The proposed IC (Fig. 2) has 4 identical HV stimulation units (SUs, STIM0-STIM3) operating in pairs to achieve TIS. Each SU has an output multiplexer to 4 electrodes, supporting a total of 16 electrodes. In principle, only 2 SUs and a more complex multiplexer could suffice. However, due to the high current and HV requirements, the multiplexer switches and their gate drivers need to be large. Thus, the proposed approach with 4 SUs and a simpler MUX result in a smaller area. On-chip digital pseudo-sine synthesizers generate the stimulation-current control signals. Two 9-bit current-steering DACs (IDAC0-1), with programmable reference currents, produce the frequency-offset currents which are mirrored into the HV stimulators. The IDACs, which are implemented in the LV domain, operate at 1MHz to achieve sufficient frequency accuracy. To avoid excessive voltage at the electrodes, high- and low-side compliance monitoring is implemented in each SU. The proposed HV stimulator is shown in Fig. 2. The current from the LV IDACs is mirrored to either CS_N or CS_P based on whether the SU is operating in sink or source mode. CS_N or CS_P are LV devices to reduce area. CS_N is protected from the HV via a regulated HV cascode M1. M1 serves a dual purpose since together with M2 it forms the output MUX. On the PMOS side, CS_P is protected via a HV cascode device. The proposed circuit only needs 11 HV devices for 4 stimulation channels (2.75 per channel). A reference-voltage-free compliance monitor with embedded HV-to-LV level shifting is proposed. When V_E is abnormally high, V_{src} is pulled towards VDDH, turning off M4 and triggering the high-side compliance flag. The low-side compliance monitor works similarly but checks the output of the regulated-cascode amplifier without the need of HV devices.

Since conventional passive CB (Fig. 3) with bulky external capacitors is impractical for 16 electrodes and unreliable for AC current stimulators [4], active CB is needed to compensate for current mismatches. While active CB solutions exist for biphasic stimulators, they generally measure residual voltages between stimuli [4-5]. Due to the semi-continuous nature of TIS, charge accumulation could reach unsafe levels during stimulation before it gets detected. For TIS, one possible approach is to monitor the common-mode voltage at the stimulator outputs and prevent it from drifting outside safe limits. However, implementing this in a power- and area-efficient way with HV compliance is not trivial. Here, we introduce an innovative active CB based on on-the-fly voltage monitoring and self-adaptive mismatch compensation (Fig. 3). First, a capacitive divider generates a scaled copy of the electrode voltage (VSEN) to enable full implementation of the voltage monitoring circuits in the LV domain. Two peak detectors, employing complementary architectures, trace and update the peak values (VPH/VPL) of VSEN within each signal cycle and extract the common-mode level (VM). VM is compared with VREF in a current-bleeding transconductor (GM) to generate 2 mismatch-compensation currents (I_P/I_N). Current-bleeding (αI_{bias}) is used to increase the transconductance and reduce the static bias current of the HV output stage. I_P/I_N are mirrored to a HV compensation-current output stage which operates in parallel with the main stimulators and is sized to handle 3σ mismatch current. An added benefit of the proposed architecture is that the extracted VPH-VPL is proportional to the ETI ($|Z_E|$). Thus, the proposed method uses the known stimulation current and VPH-VPL to derive $|Z_E|$. The proposed circuit uses only 4 HV devices per channel and offers ETI sensing during TIS without injecting any additional current that can cause artefacts.

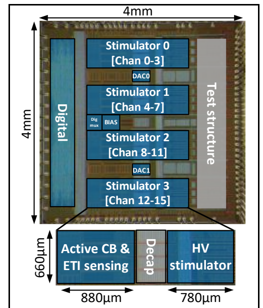

Die micrograph.

Fig. 4 shows the measurement results of a single SU. Stable currents can be supported over different voltages, and the compliance monitoring reliably triggers when compliance is not sufficient and the output current only drops by ~0.5% from its nominal value. The current mismatch is quantified at 10mA across 24 SUs from 6 different ICs (Fig. 4 top). Without CB, the measured 3σ mismatch is 103µA, which is well within the CB compensation range. Measured with an equivalent ETI model, the worst-case SFDR of the sinusoidal stimulation current is 57dB for frequencies up to 42kHz (Fig. 4 middle), providing sufficient linearity and high-frequency carriers for TIS [2]. Fig. 4 bottom shows the electrical characterization of CB and $|Z_E|$ sensing. We intentionally introduce a 3σ worst-case mismatch between the source/sink, then measured the stimulator outputs across a capacitor emulating the ETI. Without CB, the voltages drift out of compliance within 200ms. With CB, the common-mode drift reduces to <10mV/s, indicating an equivalent RMS mismatch current of <10nA. The system can also effectively measure impedances up to 1.8kΩ with an error of ≤2Ω after performing a 2-point calibration.

Fig. 5 top shows the CB and ETI sensing with a nerve electrode in-vitro. The proposed CB approach ensures a small voltage drift over a long stimulation time (1.6s) and a low voltage offset (<50mV) that is well below the water electrolysis window. After the settling period, a consistent VPH-VPL is established for ETI sensing. Fig. 5 bottom demonstrates the steering functionality of the proposed IC in-vitro. By adjusting the stimulation-current amplitudes and electrode selection, the stimulation focal region can be steered flexibly.

Fig. 6 shows a benchmark table. This work is the only HV TIS IC with a wide programmability of stimulation current and carrier frequency. A first active CB is proposed for TIS and achieves a sub-10nA mismatch. A first ETI sensing during TIS is realized with minimal design complexity. Despite the high stimulation current and HV compliance, a small active area is also achieved for both the stimulator and CB circuitry. Thanks to these features, our IC paves the way for side-effect-free neuromodulation therapies.

References:

[1] A. Fitchett et al., “Selective Neuromodulation of the Vagus Nerve,” Frontiers in Neuroscience, 2021

[2] N. Grossman et al., “Noninvasive Deep Brain Stimulation via Temporally Interfering Electric Fields,” Cell, 2017

[3] J. Xu et al., ISSCC, 2023

[4] N. Butz et al., JSSC, 2018

[5] H. Pu, et al., JSSC, 2022

[6] A. Mandal et al., CICC 2021

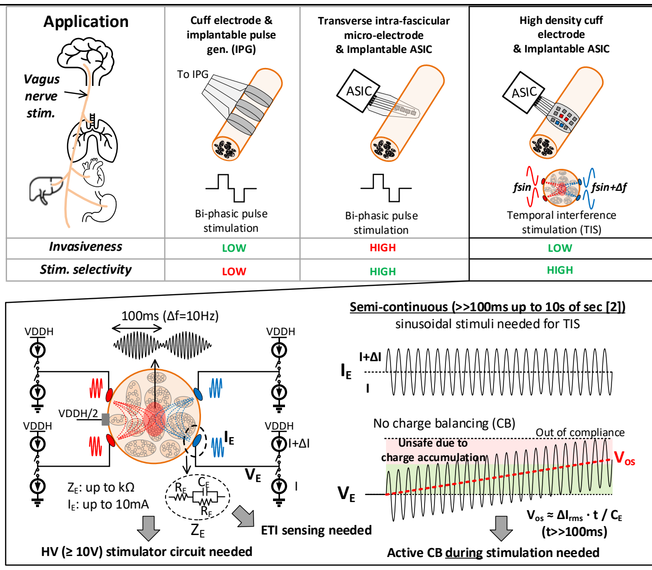

Fig. 1. Comparisons between different approaches for vagus nerve stimulation and challenges in ASIC design employing TIS.

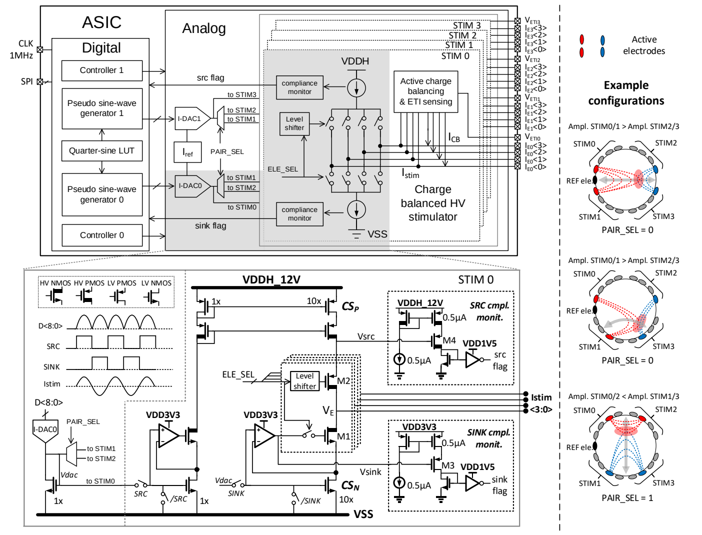

Fig. 2. (Left) ASIC architecture and HV stimulator circuit, and (right) exemplary configurations demonstrating the system can flexibly change the stimulation focal region.

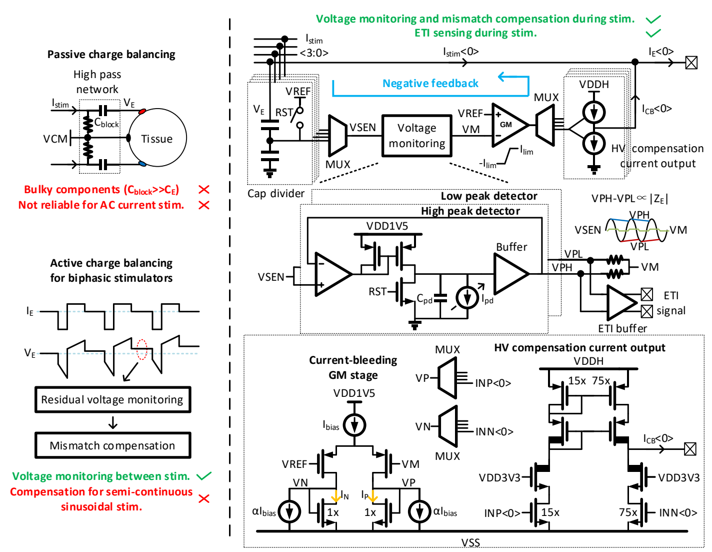

Fig. 3. (Left) Existing CB approaches, and (right) proposed CB and ETI sensing approach.

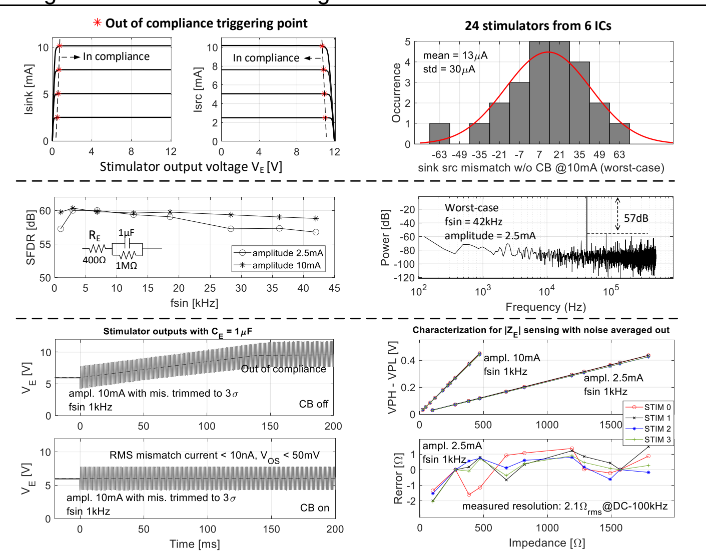

Fig. 4. (Top) Measured single stimulator DC performance without CB, (middle) AC performance with CB, and (bottom) electrical characterization of CB and $|Z_E|$ sensing.

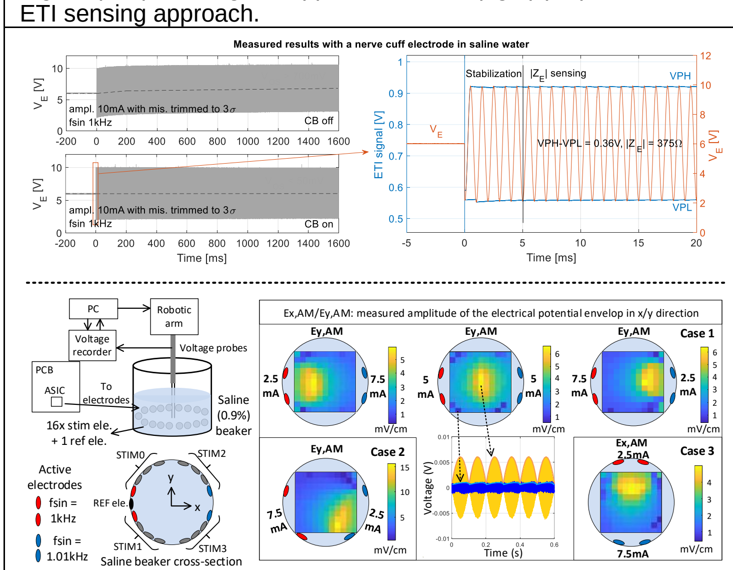

Fig. 5. (Top) in-vitro measurements of CB and ETI sensing with a nerve cuff electrode, and (bottom) in-vitro TIS demonstration with the proposed ASIC using 16 stimulation electrodes.

		This work	[3] ISSCC23	[4] JSSC18	[5] JSSC22	[6] CICC21
System	Technology	**130nm BCD**	65nm	350nm HV	180nm HV	180nm HV
	Application	**VNS**	PNS	PNS	Brain stim.	Brain stim.
	Selective stim.	**Yes**	Yes	No	No	Yes
	Stim. method/ waveform	**TIS/ Sinusoidal**	TIS/ Sinusoidal	Unipolar/ Bi-phasic	Multipolar/ Bi-phasic	Vector/ Bi-phasic
	No. channels / Stimulators	**16 / 4**	64 / 64	1 / 1	16 / 4	46 / 46
	Compliance monitor	**Yes**	No	No	No	No
Stimulator	Compliance voltage [V]	**10**	3.3	22	40	26
	DAC bit	**9b**	8b	7b	8b	7b
	Max amplitude [mA]	**10**	2	5.12	12.75	2
	Area / chan. [mm^2]	**0.13**	<0.035 [c]	1.24 [c]	0.68 [c]	0.12
	Max fsin [Hz]	**42k**	>2k	N.A.	N.A.	N.A.
	SFDR [dB]	**>57**	N.A.	N.A.	N.A.	N.A.
Charge balancing	TIS compatibility	**Yes**	N.A.	No	No	No
	CB power / SU [μW]	**63 – 128** [a]	N.A.	56	N.A.	N.A.
	Area / channel [mm^2]	**0.15**	N.A.	0.8 [c]	0.3 [c]	N.A.
	CB method	**Active**	N.A.	Active	Active	Passive
	CB precision	**$I_{mis,rms}$<10nA V_{os}<±50mV**	N.A.	V_E≲±20mV	V_E<±2mV	N.A.
ETI sensing	buffer power / SU [μW]	**54**	N.A.	N.A.	N.A.	N.A.
	Range [Ω]	**0 – 1.8k** [b]	N.A.	N.A.	N.A.	N.A.
	Inaccuracy [Ω]	**± 2** [b]	N.A.	N.A.	N.A.	N.A.
	Resolution [Ω_{rms}]	**2.1** [b]	N.A.	N.A.	N.A.	N.A.

[a] for different mismatch coverage, excluding current of HV compensation current output, which is part of stim current
[b] @stimulation amplitude of 2.5mA [c] Estimated from the die photo

Fig. 6. Benchmark table.